

The method of images revisited: Approximate solutions in wedge-shaped aquifers of arbitrary angle

Iraklis A Nikolettos¹ and Konstantinos L Katsifarakis¹

¹Aristotle University of Thessaloniki

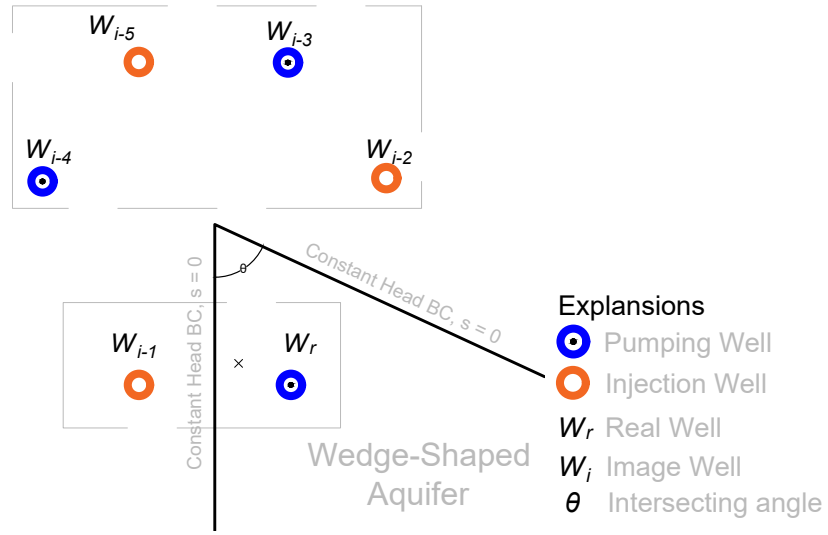
January 20, 2023

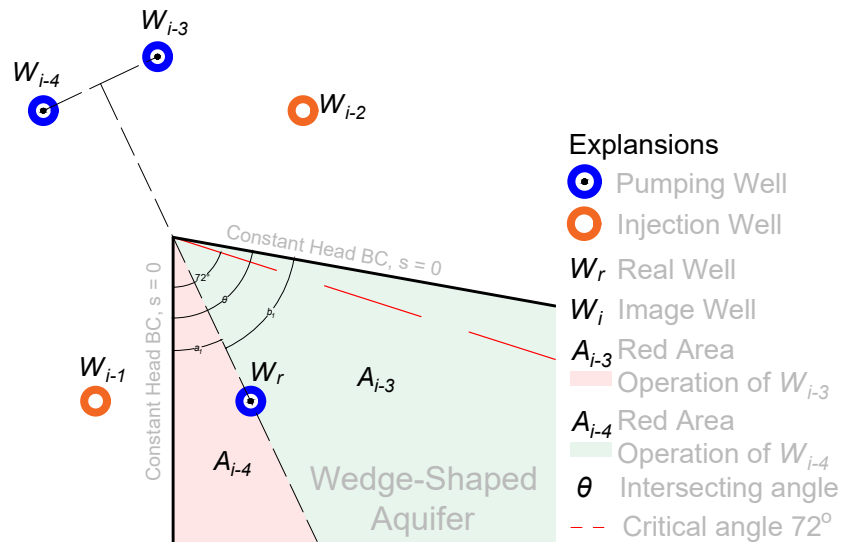
Abstract

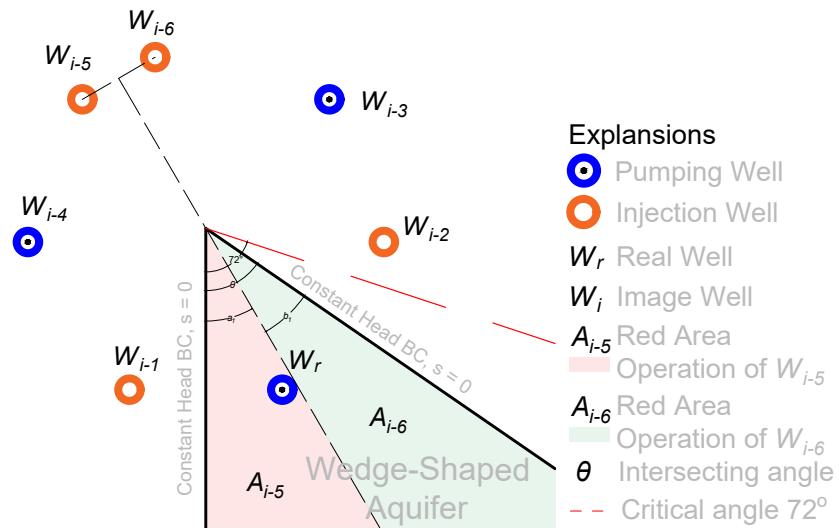
This paper focuses on deriving new approximate analytical solutions in wedge-shaped aquifers. The proposed methodology is applicable to any type of aquifer namely, leaky, confined and unconfined, under both steady state and transient flow conditions. By applying the method of images and separating the flow field into sections using physical arguments, analytical expressions are obtained for the drawdown function. In contrast to the conventional theory, the proposed solutions are applicable to arbitrary wedge angle. Comparison of the results of the derived approximate analytical solutions to numerical ones, is considered necessary to ensure its validity. MODFLOW, a well-known numerical tool is used to calculate the numerical results. The results indicate that the boundary conditions are fully observed, the drawdown is feasible to be calculated at any point of the real flow field (continuity of the drawdown function) and discrepancies compared to numerical results are considered negligible. The main advantage of the proposed procedure is that it can be easily used in conjunction with meta-heuristic algorithms to solve groundwater resources optimization problems.

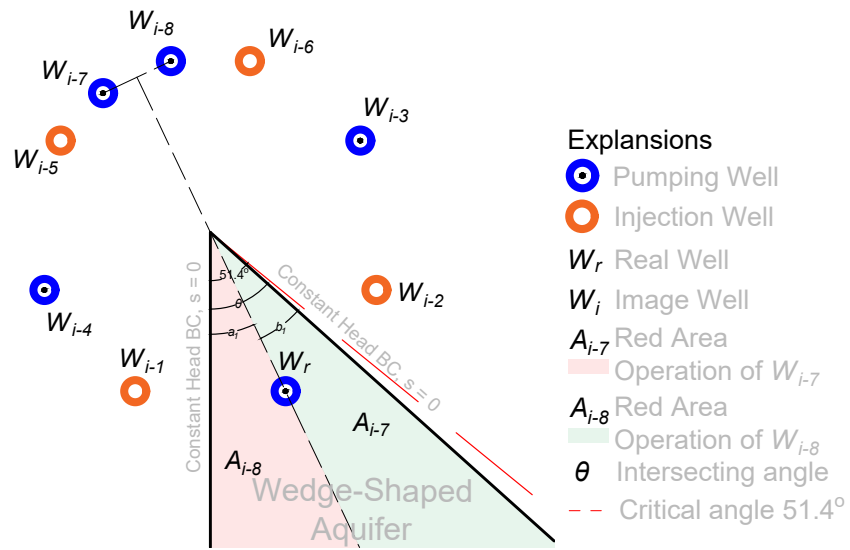
Hosted file

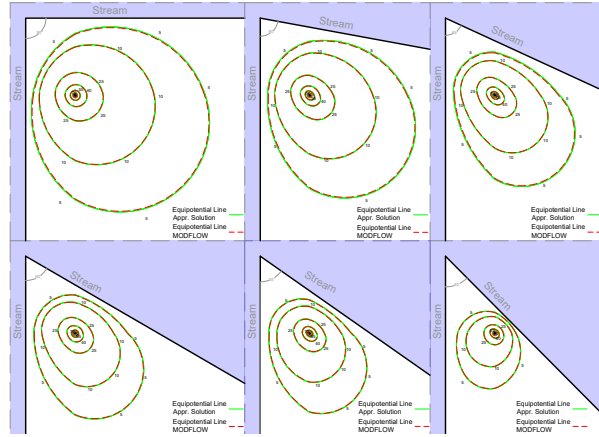
952658_0_art_file_10556125_rnwtj4.docx available at <https://authorea.com/users/577697/articles/619973-the-method-of-images-revisited-approximate-solutions-in-wedge-shaped-aquifers-of-arbitrary-angle>











22 the proposed procedure is that it can be easily used in conjunction with meta-heuristic algorithms
23 to solve groundwater resources optimization problems.

24

25 **Keywords**

26 Wedge-shaped aquifers; method of images; groundwater flow; approximate analytical solutions;
27 MODFLOW; Well function

28

29 **1. Introduction**

30 Aquifers bounded by two boundaries, constant head such as streams and lakes or no flux, such as
31 impermeable rocks, intersecting at angle smaller than 90° are called wedge-shaped (Mahdavi,
32 2021). Their study has been the subject of research interest over the years. Most of the research
33 papers were focused on analytical, approximate analytical and semi-analytical expressions for
34 drawdown calculation and estimation of the aquifer's parameters (Singh, 2001; Yeh et. al.,
35 2008).

36 Analytical procedures have been followed in several research papers to obtain expressions for
37 the drawdown function. The well-known Hankel transform has been used by Chan et. al. (1978),
38 Yeh et. al. (2006) and Chuang and Yeh (2018) to obtain analytical solutions in wedge-shaped
39 aquifers under steady state and transient flow conditions respectively. Chen et. al. (2009) have
40 applied the method of images to describe the aquifer's response to a constant pumping well.
41 Other methods used to derive analytical solutions to wedge-shaped aquifers are the revisited
42 Strack-Chernysov model (Kacimov et.al., 2016), fractional calculus (Kavvas et. al., 2017) and
43 Laplace transform (Lin et. al., 2018). Recently, more complicated aquifer's shapes, such as

44 triangle-shaped, annular wedge-shaped, trapezoidal-shaped, have been studied analytically
45 (Asadi-Aghbolaghi & Seyyedean, 2010; Kacimov et. al., 2017; Leray et. al., 2019; Mahdavi,
46 2019; Mahdavi and Yazdani, 2021; Mahdavi, 2022; Nagheli et. al., 2020; Zlotnik et. al., 2015).

47 When no analytical solutions are available, semi-analytical and approximate analytical methods
48 have been adopted to investigate wedge-shaped aquifers. Dimensionless type curves of flux-time
49 and drawdown-time are given for homogeneous aquifers by Sedghi et. al. (2010) and Sedghi et.
50 al. (2012) as well as for heterogeneous ones from Samani and Sedghi (2015), using integrals
51 transform methods. Wang et al. (2018) presented a Laplace transform boundary element method
52 to simulate the groundwater flow. Estimation of hydraulic parameters and prediction of the
53 discharge of qanat in alluvial aquifers is achieved via the semi-analytical approach introduced by
54 Sedghi and Zhan (2022). On the other hand, approximate analytical solutions are simplified
55 expressions aiming to describe complex problems with good accuracy. Approximate solutions to
56 Forcheimer equation (Moutsopoulos & Tsihrintzis, 2005; Okuyade et. al., 2022)) and
57 groundwater response to tidal fluctuations (Monachesi & Guarracino, 2011) are only a few
58 examples showing their usefulness. Expressions obtained from approximate procedures suit
59 perfectly to be used in combination with meta-heuristic methods (Christelis et. al., 2019;
60 Karpouzou & Katsifarakis 2021; Mallios et. al., 2022; Rodriguez-Pretelin & Nowak 2019).
61 Further discussion about approximate analytical solutions will follow in section 3.

62 In this framework, approximate analytical solutions for wedge-shaped aquifers are sought.
63 Observance of boundary conditions, either constant head or no flux, as well as continuity of the
64 drawdown function were set as prerequisites. The concept of the proposed methodology is the
65 division of the real flow field into two sections, where different fictitious wells are taken into

66 account. The method of images has been applied to introduce the fictitious, pumping or injection
67 wells.

68 **2. Outline of the method of images**

69 The basic concept of the method of images is that a boundary can be “removed” by adding a
70 number of fictitious (or image) wells, symmetrical of the real ones with respect to it, resulting
71 into an equivalent infinite flow field (Haitjema, 2006; Mahdavi, 2020; Nikoletos, 2020). The
72 sign of the flow rate of each image well depends on the boundary condition and guarantees its
73 observance (Katsifarakis et al., 2018; Samani & Zarei-Doudeji, 2012). From mathematical point
74 of view, it is a specific application of the Green’s function and is applicable to problems
75 described by the Poisson equation (Mohamed & Paleologos, 2018). Its use is extensive in many
76 scientific fields such as groundwater hydraulics (Kuo et. al., 1994), electrostatics (Nguyen &
77 Mehrabian, 2021), magnetics (Curtis et. al., 2015) and optics. The method of images has been
78 widely used in groundwater flow simulation problems to calculate hydraulic head level
79 drawdown (Atangana, 2014; Nikoletos & Katsifarakis, 2022; Penny et. al., 2020), to describe
80 interaction between ground and surface water (Anderson, 2003) and to optimize the management
81 of aquifers (Katsifarakis, 2008) and especially coastal aquifers facing saltwater intrusion
82 problems (Etsias et. al., 2021; Mantoglou, 2003). It is worth mentioning that the method of
83 images gives exact solutions in wedge-shaped aquifers bounded by two boundaries intersecting
84 at angles of : 90° , 60° , 45° , 30° etc. (each angle verifying eq. 1)

$$85 \quad \theta = \frac{360^\circ}{N+1}, \quad N = 3, 5, 7, \dots$$

86 (1)

87 Where θ , is the boundary intersection angle and N, the number of fictitious wells.

88

89

90

91 **3. Approximate analytical solutions**

92 **3.1 Previous Studies**

93 Due to the complexity of many flow fields, exact solutions cannot be found. In such cases,
94 approximate analytical solutions could be a good alternative, if the introduced error is acceptable
95 and the computational volume low. On the other hand, solutions produced by numerical methods
96 are inherently approximate, too. Convergence of both approximate analytical and numerical
97 methods point out the validity of the proposed solutions.

98 In the following paragraphs, the usefulness of approximate analytical solutions to groundwater
99 resources management problems is presented. Drawdown distribution in semi-infinite aquifers is
100 easily calculated via approximate solutions (Nikoletos & Katsifarakis, 2022; Sun et. al., 2011;
101 Zlotnik et. al., 2017; Yang et. al., 2014). Accurate calculation of stream depletion rate due to
102 pumping wells located at adjacent aquifers is another scientific issue where approximate
103 solutions have been a valuable asset (Huang & Yeh, 2015; Huang et. al., 2018; Lapidés et. al.,
104 2022; Smerdon et. al., 2012 ; Teloglou & Bansal, 2012; Zipper et al., 2019). Their combination
105 with heuristic methods to groundwater optimization problems reveal the ability to keep the
106 computational load much smaller in comparison with numerical ones (Christelis & Mantoglou,
107 2019).

108 **3.2 Basic concept of the proposed solutions**

109 The aim of the proposed solutions is to calculate with good accuracy the drawdown distribution
110 in a wedge-shaped flow field, while observing the boundary conditions. Following the approach
111 developed by Nikoletos and Katsifarakis (2022), we divided the real flow field into two sections.
112 In each section a number of fictitious wells are used in a way that observance of the boundary
113 conditions is achieved. The proposed division of the flow field in two sections, does not disrupt
114 continuity of the drawdown, but the flow velocity field is discontinuous, along the straight line
115 that separates the field.

116 The accuracy of the results as well as the applicability range of the proposed approximate
117 solutions are discussed in the following sections.

118 **3.3 Comparison with previous studies**

119 Kuo et. al. (1994) proposed a new approach for predicting drawdown in aquifer with irregularly
120 shaped boundaries using the image well method. More recently, a novel methodology for
121 estimation of stream filtration from a meandering stream, is introduced by Huang and Yeh
122 (2015) by applying image well theory. In both papers the decision variables were the flow rates
123 of the image wells which are determined by solving a system of equations. In this paper the
124 decision variables are the number of fictitious wells taking into account the physical
125 interpretation of the method. The proposed methodology is more suitable to problems where the
126 intersecting boundaries are straight lines while the aforementioned methods are preferred where
127 the boundaries are curved. It is worth mentioning that combination of the method proposed by
128 Nikoletos and Katsifarakis with the method introduced by Kuo et. al. (1994) or Huang and Yeh
129 (2015) could lead to more accurate results for the calculation of the drawdown. This will be an
130 issue of future study.

131 3.4 Structure of the drawdown function

132 The proposed methodology can be applied to any type of aquifer under steady state and transient
133 flow conditions. The drawdown functions at any point (x,y) , due to pumping from a single well,
134 in confined, unconfined and leaky aquifers are given by the following relationships respectively
135 (Theim, 1906):

$$136 \quad s(x, y) = -\frac{1}{2\pi T} Q_w \ln \frac{\sqrt{(x-x_w)^2+(y-y_w)^2}}{R} \quad (2.a)$$

$$137 \quad s(x, y) = \frac{1}{2\pi T} Q_w K_o \left(\frac{\sqrt{(x-x_w)^2+(y-y_w)^2}}{L} \right) \quad (2.b)$$

$$138 \quad H^2 = H_1^2 + \frac{1}{\pi K} Q_w \ln \frac{\sqrt{(x-x_w)^2+(y-y_w)^2}}{R} \quad (2.c)$$

139 Where, Q_w is the flow rate of the well, (x_w, y_w) are the well's coordinates, K is the hydraulic
140 conductivity, T is the aquifer's transmissivity, R is the radius of influence, L is the leaky
141 coefficient, K_o is the modified Bessel function of second kind and zero order and H and H_1 are
142 the distances between water table and initial water table and a reference level.

143 To demonstrate the procedure, we consider steady flow in confined aquifers.

144 3.4.1 Intersecting angle – Case of $90^\circ < \theta < 60^\circ$

145 In the following paragraphs, we present solutions for wedge-shaped aquifers where the
146 boundaries are both of constant head or impermeable. We demonstrate the proposed
147 methodology for constant head boundaries. The process is the same in case of impermeable
148 boundaries, except the kind of the fictitious wells.

149 The exact solution for the drawdown due to a pumping well in flow fields bounded by two
150 boundaries intersecting at angle 90° and 60° makes use of 3 and 5 fictitious wells, respectively.

151 Based on that, we postulate that the proposed solutions should make use of 3 to 5 fictitious wells.
152 As shown in Fig. 3, W_{i-1} and W_{i-2} are the images of the real well with respect to the closest and
153 the furthest boundary respectively; we call them first-order images. W_{i-3} and W_{i-4} are the images
154 of W_{i-1} and W_{i-2} with respect to the other boundary; we call them second-order images. W_{i-5} and
155 W_{i-6} , resulting in a similar way, are the third-order images, and so on. The odd order images of a
156 pumped well are injection wells, while the even order ones represent pumping wells.

157 From the physical point of view, the influence of the image wells should decrease, as their order
158 increases. For instance, the first order images should affect more the conditions in the real flow
159 field, namely they should be located closer to it than the second order ones, the second order
160 images should be closer to the real flow field than the third order ones and so on. The largest
161 order image wells should operate alternately in parts of the flow field, in order to satisfy the
162 boundary conditions. According to the geometrical proof found in Appendix A, if the angle θ is
163 larger than 72° , the third order images are closer to the real flow field than the second order ones.
164 Consequently, we conclude that for angles larger than 72° , 3 fictitious wells should be used,
165 while for angles smaller than 72° , 5 fictitious wells should be used, provided that the conditions
166 described by inequalities (8) and (9) of Appendix A are also satisfied. Otherwise the largest
167 order images should not be used.

168 From the physical point of view, we expect that the drawdown at any point of the real flow field
169 decreases as the angle between the boundaries decreases. According to Fig. 1, by isolating W_r
170 and W_{i-1} results into conditions equal to one constant head boundary. The second constant head
171 boundary should further reduce the drawdown. Therefore the system of W_{i-2} , W_{i-3} , W_{i-4} and W_{i-5}
172 or W_{i-6} (for the respective system of W_r and W_{i-2}) should represent the influence of the second
173 boundary. This reduction depends on the distance of the above mentioned system from the real

174 flow field. As the angle θ increases, the system of the image wells diverges from the real flow
 175 field, so its influence decreases, too.

176 **Fig. 1.** Separation of the wells into two groups. *Note:* BC stands for boundary condition.

177 Therefore, the following two-branch functions could describe the drawdown distribution to the
 178 real flow field in each case.

179 For $90^\circ > \theta > 72^\circ$

$$180 \quad s(x, y) = \begin{cases} -\frac{1}{2\pi T} Q_w \ln \frac{\sqrt{(x-x_w)^2+(y-y_w)^2} \sqrt{(x-x_{w4})^2+(y-y_{w4})^2}}{\sqrt{(x-x_{w1})^2+(y-y_{w1})^2} \sqrt{(x-x_{w2})^2+(y-y_{w2})^2}} \\ -\frac{1}{2\pi T} Q_w \ln \frac{\sqrt{(x-x_w)^2+(y-y_w)^2} \sqrt{(x-x_{w3})^2+(y-y_{w3})^2}}{\sqrt{(x-x_{w1})^2+(y-y_{w1})^2} \sqrt{(x-x_{w2})^2+(y-y_{w2})^2}} \end{cases} \quad (3)$$

181 **Fig. 2.** Wedge-shaped aquifer $90^\circ > \theta > 72^\circ$

182

183 For $72^\circ > \theta > 60^\circ$

$$184 \quad s(x, y) = \begin{cases} -\frac{1}{2\pi T} Q_w \ln \frac{\sqrt{(x-x_w)^2+(y-y_w)^2} \sqrt{(x-x_{w3})^2+(y-y_{w3})^2} \sqrt{(x-x_{w4})^2+(y-y_{w4})^2}}{\sqrt{(x-x_{w1})^2+(y-y_{w1})^2} \sqrt{(x-x_{w2})^2+(y-y_{w2})^2} \sqrt{(x-x_{w5})^2+(y-y_{w5})^2}} \\ -\frac{1}{2\pi T} Q_w \ln \frac{\sqrt{(x-x_w)^2+(y-y_w)^2} \sqrt{(x-x_{w3})^2+(y-y_{w3})^2} \sqrt{(x-x_{w4})^2+(y-y_{w4})^2}}{\sqrt{(x-x_{w1})^2+(y-y_{w1})^2} \sqrt{(x-x_{w2})^2+(y-y_{w2})^2} \sqrt{(x-x_{w6})^2+(y-y_{w6})^2}} \end{cases} \quad (4)$$

185

186 **Fig. 3.** Wedge-shaped aquifer $72^\circ > \theta > 51.4^\circ$

187

188 3.4.2 Intersecting angle – Case of $60^\circ > \theta > 45^\circ$

189 If the intersecting angle of the boundaries is 60° , the exact analytical solution makes use of 5
 190 fictitious wells. If the angle is 45° , 7 fictitious wells are placed to the equivalent infinite flow

191 field. We postulate, then, that the proposed approximate solutions should make use of 5 to 7
 192 fictitious wells. The main difference compared to the case 90° - 60° is that the largest order images
 193 are pumping wells. Taking into account the physical interpretation of the aquifer's response, the
 194 4th order images should be located farther than the 3rd order ones from the real flow field.

195 According to the geometrical proof found in Appendix A, if the angle is larger than 51.42° , the
 196 4th order images are closer to the real flow field than the 3rd order ones. The largest order image
 197 wells should be used alternately in parts of the flow field, in order to ensure the observance of
 198 boundary conditions. Consequently, we conclude that for angles larger than 51.42° we should use
 199 5 fictitious wells, while for angles smaller than 51.42° , 7 fictitious wells should be used,
 200 provided that the conditions described by inequalities (8) and (9) of Appendix A are also
 201 satisfied. Otherwise the largest order images should not be used.

202 Verification of the drawdown reduction as the angle θ decreases is needed. We examine
 203 separately W_r and W_{i-1} and rest of the wells. According to Section 3.4.1 the system of wells W_{i-2} ,
 204 W_{i-3} , W_{i-4} , W_{i-5} or W_{i-6} (for the respective system of W_r and W_{i-2}) offers water quantity to the real
 205 flow field. Consequently, it 's proved that W_{i-5} and W_{i-6} are closer to the real flow field than W_{i-7}
 206 and W_{i-8} , respectively. According to the geometrical proof of Appendix A, the aforementioned
 207 conditions holds.

208 Hence, the following two-branch functions describe the drawdown distribution to the real flow
 209 field in each case.

210 For $60^\circ > \theta > 51.42^\circ$

$$211 \quad s(x, y) = \begin{cases} -\frac{1}{2\pi T} Q_w \ln \frac{\sqrt{(x-x_w)^2+(y-y_w)^2}\sqrt{(x-x_{w3})^2+(y-y_{w3})^2}\sqrt{(x-x_{w4})^2+(y-y_{w4})^2}}{\sqrt{(x-x_{w1})^2+(y-y_{w1})^2}\sqrt{(x-x_{w2})^2+(y-y_{w2})^2}\sqrt{(x-x_{w5})^2+(y-y_{w5})^2}} \\ -\frac{1}{2\pi T} Q_w \ln \frac{\sqrt{(x-x_w)^2+(y-y_w)^2}\sqrt{(x-x_{w3})^2+(y-y_{w3})^2}\sqrt{(x-x_{w4})^2+(y-y_{w4})^2}}{\sqrt{(x-x_{w1})^2+(y-y_{w1})^2}\sqrt{(x-x_{w2})^2+(y-y_{w2})^2}\sqrt{(x-x_{w6})^2+(y-y_{w6})^2}} \end{cases} \quad (5)$$

212 It is worth mentioning that in this case and the case of $90^\circ > \theta > 72^\circ$ the number of fictitious
 213 wells coincides.

214

215 For $51.42^\circ > \theta > 45^\circ$

$$216 \quad s(x, y) = \begin{cases} -\frac{1}{2\pi T} Q_w \ln \frac{\sqrt{(x-x_w)^2+(y-y_w)^2} \sqrt{(x-x_{w3})^2+(y-y_{w3})^2} \sqrt{(x-x_{w4})^2+(y-y_{w4})^2} \sqrt{(x-x_{w8})^2+(y-y_{w8})^2}}{\sqrt{(x-x_{w1})^2+(y-y_{w1})^2} \sqrt{(x-x_{w2})^2+(y-y_{w2})^2} \sqrt{(x-x_{w5})^2+(y-y_{w5})^2} \sqrt{(x-x_{w6})^2+(y-y_{w6})^2}} \\ -\frac{1}{2\pi T} Q_w \ln \frac{\sqrt{(x-x_w)^2+(y-y_w)^2} \sqrt{(x-x_{w3})^2+(y-y_{w3})^2} \sqrt{(x-x_{w4})^2+(y-y_{w4})^2} \sqrt{(x-x_{w7})^2+(y-y_{w7})^2}}{\sqrt{(x-x_{w1})^2+(y-y_{w1})^2} \sqrt{(x-x_{w2})^2+(y-y_{w2})^2} \sqrt{(x-x_{w5})^2+(y-y_{w5})^2} \sqrt{(x-x_{w6})^2+(y-y_{w6})^2}} \end{cases} \quad (6)$$

217 **Fig. 4. Wedge-shaped aquifer $51.4^\circ > \theta > 45^\circ$**

218

219 **3.4.3 Intersecting angle – Cases of $\theta < 45^\circ$**

220 For the rest of the cases, we follow exactly the same methodology as described in sections 3.4.1
 221 and 3.4.2, for consecutive analytical solutions. The determination of the critical angle of each
 222 case as well as the operating wells of each section are based on eq. 11 and Fig. 6, found in
 223 Appendix A.

224 **4. Evaluation through comparison with numerical simulation results**

225 MODFLOW (Harbaugh, 2005; Harbaugh et. al., 2017), an established, finite-difference,
 226 groundwater flow simulation model is used for numerical evaluation of the proposed solutions. It
 227 is widely used by hydrogeologists to simulate real and theoretical flow fields for estimation of
 228 the response of the aquifers (Malekzadeh et. al., 2019). The program has been applied

229 extensively to aquifers bounded by two or more irregular shaped boundaries (Aghlmand and
230 Abbasi, 2019; Karimi et. al., 2019).

231

232 Here we use MODFLOW to evaluate the quality of the proposed approximate solutions. We
233 consider 6 cases of wedge-shaped aquifers, bounded by two constant head boundaries,
234 intersecting at the point O (0, 2000). One boundary is described by the equation $x = 0$. A well
235 with coordinates (320, 1500) pumps at a flow rate $Q_w = 0.02 \text{ m}^3/\text{s}$. The hydraulic parameters of
236 the well and the aquifer are listed below.

237 a) Radius of the well $r_0 = 0.5 \text{ m}$

238 b) Hydraulic Conductivity $K = 0.0000016 \text{ m/s}$

239 c) Thickness of aquifer $a = 100 \text{ m}$

240 We consider steady-state flow conditions to facilitate the comparison with the approximate
241 analytical solutions.

242 A grid of $5 \times 5 \text{ m}$ has been used to run MODFLOW and the results have been compared to those
243 obtained from the approximate analytical solutions. Visualization of the results has been made
244 through ModelMuse (Winston, 2009; Winston, 2020), a well-known graphical user interface for
245 groundwater simulation models. The results for 6 θ values are discussed in the following
246 paragraphs.

247 For $\theta=90^\circ$, 60° and 45° the solutions are exact. These cases serve rather to check MODFLOW
248 results. The analytical solutions give slightly larger values than MODFLOW. Discrepancies are
249 smaller than 5% at all points of the real flow field except the location of the well.

250 For $\theta=80^\circ$, 65° and 55° the solutions are approximate. The approximate analytical solutions
251 render larger drawdown values than MODFLOW. Discrepancies are smaller than 6% at all
252 points of the real flow field except the location of the well.

253 Equipotential lines, obtained by the two methods, are shown in Fig. 5

254 **Fig. 5.** Equipotential lines for different boundary intersection angles obtained by approximate solution and
255 MODFLOW

256 **5. Conclusions and Discussion**

257 New functions for the calculation of the drawdown distribution of wedge-shaped aquifers via
258 approximate analytical procedures are presented, based on the method of images. Observance of
259 the boundary conditions is achieved through the use of two-branch functions. The largest order
260 fictitious wells are activated alternately in parts of the flow field. The division of the flow field in
261 two sections does not disrupt continuity of the drawdown. The only drawback is that the flow
262 velocity field is discontinuous, along the straight line that separates the field.

263 To check the validity of the approximate solutions, results for six application examples have
264 been compared to numerical ones, obtained by MODFLOW. For θ equal to 90° , 60° and 45° ,
265 namely when the method of images is exact, the discrepancies are generally smaller than 5%,
266 while in the other cases, discrepancies are generally smaller than 6%. The main advantage of the
267 proposed solutions is that the respective computational load is low, so they can be easily used in
268 conjunction with meta-heuristic algorithms to solve groundwater resources optimization
269 problems.

270 **Open Research Section**

271 **Data Availability Statement**

272 The paper is purely theoretical. Data were not used, nor created for this research.

273 **Software Availability Statement**

274 Software for this research is available through <https://zenodo.org/record/7501194>

275 **Appendix A: Geometrical Proof**

276 Let angle θ be between two consecutive angles, namely θ_k and θ_{k-2} where the image well method
277 is exact and the number of fictitious wells is k and $k-2$ respectively.

278 Let a and b be the angles of OW_r with the field boundaries Ox_1 and Ox_2 respectively.

279 Let angle c be given by the following equation:

$$280 \left(\frac{k+(k-2)}{4}\right)\theta + c = 180^\circ \Rightarrow c = 180^\circ - \left(\frac{k+(k-2)}{4}\right)\theta$$

281 (7)

282 If the angle $\theta = (Ox_1, Ox_2) < \frac{360^\circ}{k}$, the penultimate order image $W_{i-(k-2)}$ is closer than the last-
283 order image W_{i-k} to W_r and to any point of the real field.

284 Proof: If $b < c$, then $(Ox_2, W_{i-2}) < c$, namely W_{i-2} lies on the same side of Ox_n , with W_r .

285 Consequently, W_{i-4} , the image well of W_{i-2} with respect to Ox_1 lies under the side of Ox_{n+1} . Since

286 Ox_2 is the bisector of Ox_1' and Ox_{n+1}' , the image well of W_{i-4} with respect to Ox_2 , namely W_{i-6} ,

287 lies on the opposite site of Ox_1 . The same condition holds for the consecutive mirror wells with

288 respect to the corresponding boundary until the penultimate well, namely $W_{i-(k-2)}$. For the last

289 order image well, Ox_1 is the perpendicular bisector of $W_{i-(k-2)}$ and W_{i-k} . Therefore $W_{i-(k-2)}$ and W_{i-k}

290 lie on the opposite site of Ox_1 . As shown in Fig. 6 the following relationships hold:

$$291 b < c$$

292 (8)

293 $a < c$

294 (9)

295 Also, we take advantage of the following property

$$296 \quad a + b = \theta \Rightarrow b = \theta - a \quad (10)$$

297 Adding up the inequalities (8) and (9) resulting

$$a + b < 2c \xrightarrow{(7)-(10)} \theta < 2 \left(180^\circ - \left(\frac{k + (k - 2)}{4} \right) \theta \right) \Rightarrow \theta < 360^\circ - (k - 1)\theta \Rightarrow k\theta < 360^\circ$$

$$298 \quad \Rightarrow \theta < \frac{360^\circ}{k}$$

299 (11)

300 **Fig. 6.** Geometrical relationships between real and fictitious wells for arbitrary wedge angle.

301

302 **References**

303

- 304 1. Aghlmand, R. and Abbasi, A. (2019) “Application of MODFLOW with Boundary
305 Conditions Analyses Based on Limited Available Observations: A Case Study of Birjand
306 Plain in East Iran”. **Water**, 11(9), <https://doi.org/10.3390/w11091904>
- 307 2. Anderson, E.I. (2003) “An analytical solution representing groundwater–surface water
308 interaction”. **Water Resources Research**, 39(3), <https://doi.org/10.1029/2002WR001536>
- 309 3. Asadi-Aghbolaghi, M. and Seyyedian, H. (2010) “An analytical solution for groundwater
310 flow to a vertical well in a triangle-shaped aquifer”. **Journal of Hydrology**, 393(3-4):341-
311 348, <https://doi.org/10.1016/j.jhydrol.2010.08.034>

- 312 4. Atangana, A. (2014) “Drawdown in prolate spheroidal–spherical coordinates obtained via
313 Green’s function and perturbation methods”. **Communications in Nonlinear Science and**
314 **Numerical Simulation**, 19(5):1259-1269, <https://doi.org/10.1016/j.cnsns.2013.09.031>
- 315 5. Chan, Y.K., Mullineaux, N., Reed, J.R. and Wells, G.G. (1978) “Analytic solutions for
316 drawdowns in wedge-shaped artesian aquifers”. **Journal of Hydrology**, 36(3-4):233-246,
317 [https://doi.org/10.1016/0022-1694\(78\)90146-4](https://doi.org/10.1016/0022-1694(78)90146-4)
- 318 6. Chen, Y.J., Yeh, H.D. and Yang, S.Y. (2009) “Analytical Solutions for Constant-Flux and
319 Constant-Head Tests at a Finite-Diameter Well in a Wedge-Shaped Aquifer”. **Journal of**
320 **Hydrologic Engineering**, 135(4), [https://doi.org/10.1061/\(ASCE\)0733-](https://doi.org/10.1061/(ASCE)0733-9429(2009)135:4(333))
321 [9429\(2009\)135:4\(333\)](https://doi.org/10.1061/(ASCE)0733-9429(2009)135:4(333))
- 322 7. Christelis, V., Kopsiaftis, G. and Mantoglou, A. (2019) “Performance comparison of
323 multiple and single surrogate models for pumping optimization of coastal aquifers”,
324 **Hydrological Sciences Journal**, 64(3) <https://doi.org/10.1080/02626667.2019.1584400>
- 325
- 326 8. Christelis, V. and Mantoglou, A. (2019) “Pumping Optimization of Coastal Aquifers Using
327 Seawater Intrusion Models of Variable-Fidelity and Evolutionary Algorithms”. **Water**
328 **Resources Management**, 33:555-568, <https://doi.org/10.1007/s11269-018-2116-0>
- 329 9. Chuang, M.H. and Yeh, H.D. (2018) “An Analytical Solution of Groundwater Flow in
330 Wedge-shaped Aquifers with Estuarine Boundary Conditions.”. **Water Resources**
331 **Management**, 32:5027-5039, <https://doi.org/10.1007/s11269-018-2125-z>
- 332 10. Curtis, M., Paulides, J.H. and Lomonova, E.A. (2015) “An overview of analytical methods
333 for magnetic field computation”. **Tenth International Conference on Ecological Vehicles**
334 **and Renewable Energies (EVER)**, [10.1109/EVER.2015.7112938](https://doi.org/10.1109/EVER.2015.7112938)

- 335 11. Etsias, G., Hamill, G.A., Aguila, J.F., Benner, E.M., McDonnell, M.C., Ahmed, A.A. and
336 Flynn, R. (2021) “The impact of aquifer stratification on saltwater intrusion characteristics.
337 Comprehensive laboratory and numerical study”. **Hydrological Processes**, 35(4):14120,
338 <https://doi.org/10.1002/hyp.14120>
- 339 12. Haitjema, H. (2006) “The Role of Hand Calculations in Ground Water Flow Modeling”.
340 **Journal of Hydrology**, 36(3-4):233-246, <https://doi.org/10.1111/j.1745-6584.2006.00189.x>
- 341 13. Harbaugh, A.W., (2005) “MODFLOW-2005, the U.S. Geological Survey modular ground-
342 water-model- the Ground Water Flow Process: U.S. Geological Survey Techniques and
343 Methods 6-A16
- 344 14. Harbaugh, A.W., Langevin, C.D., Hughes, J.D., Niswonger, R.N. and Konikow, L.F.
345 (2017) “MODFLOW-2005 version 1.12.00, the U.S. Geological Survey modular
346 groundwater model”. U.S. Geological Survey Software Release, 03 February 2017,
347 <http://dx.doi.org/10.5066/F7RF5S7G>
- 348 15. Huang, C.S. and Yeh, H.D. (2015) “Estimating stream filtration from a meandering stream
349 under the Robin condition”. **Water Resources Research**, 51, 4848-4857,
350 <https://doi.org/10.1002/2015WR016975>
- 351 16. Huang, C.S., Yang, T. and Reed, Yeh, H.D. (2018) “Review of analytical models to stream
352 depletion induced by pumping: Guide to model selection”. **Journal of Hydrology**,
353 561:277-285, <https://doi.org/10.1016/j.jhydrol.2018.04.015>
- 354 17. Kacimov, A.R., Kayumov, I.R. and Al-Maktoumi, A. (2016) “Rainfall induced
355 groundwater mound in wedge-shaped promontories: The Strack–Chernyshov model
356 revisited”. **Advances in Water Resources**, 97:110-119,
357 <https://doi.org/10.1016/j.advwatres.2016.08.011>

- 358 18. Kacimov, A.R., Maklakov, D.V. and Kayumov, I.R.. (2017) “Free Surface Flow in a
359 Microfluidic Corner and in an Unconfined Aquifer with Accretion: The Signorini and
360 Saint-Venant Analytical Techniques Revisited”. **Transport in Porous Media**, 116:115-
361 142, <https://doi.org/10.1007/s11242-016-0767-y>
- 362 19. Karimi, L., Motagh, T. and Entezam, I. (2019) “Modeling groundwater level fluctuations in
363 Tehran aquifer: Results from a 3D unconfined aquifer model”. **Groundwater for
364 Sustainable Development**, 8:439-449, <https://doi.org/10.1016/j.gsd.2019.01.003>
- 365 20. Karpouzou, D.K. and Katsifarakis, K.L. (2021) “A new benchmark optimization problem of
366 adaptable difficulty: theoretical considerations and practical testing”. **Operational
367 Research**, 21:231-250, <https://doi.org/10.1007/s12351-019-00462-8>
- 368 21. Katsifarakis, K.L. (2008) “Groundwater pumping cost minimization-An analytical
369 approach”. **Water Resources Management**, 22(8):1089-1099,
370 <https://doi.org/10.1007/s11269-007-9212-x>
- 371 22. Katsifarakis, K.L., Nikolettos, I.A. and Stavridis, C. (2018) “Minimization of Transient
372 Groundwater Pumping Cost - Analytical and Practical Solutions”. **Water Resources
373 Management**, 32:1053-1069, <https://doi.org/10.1007/s11269-017-1854-8>
- 374 23. Kavvas, M.L., Tu, T., Ercan, A. and Polsinelli, J. (2017) “Fractional governing equations of
375 transient groundwater flow in confined aquifers with multi-fractional dimensions in
376 fractional time”. **Earth System Dynamics**, 8:921-929, [https://doi.org/10.5194/esd-8-921-
377 2017](https://doi.org/10.5194/esd-8-921-2017)
- 378 24. Kuo, M.C.T., Wang, W.L., Lin, D.S. and Chiang, C.J. (1994) “An Image-Well Method for
379 Predicting Drawdown Distribution in Aquifers with Irregularly Shaped Boundaries”.
380 **Groundwater** Vol. 32(5), 794-804, <https://doi.org/10.1111/j.1745-6584.1994.tb00921.x>

- 381 25. Lapiques, D.A., Maitland, B.M., Zipper, S.C., Latzka, A.W., Pruitt, A. and Greve, R. (2022)
382 “Advancing environmental flows approaches to streamflow depletion management”.
383 **Journal of Hydrology**, 607:127447, <https://doi.org/10.1016/j.jhydrol.2022.127447>
- 384 26. Leray, S., Gauvain, A. and Dreuzy, J.R. (2019) “Residence time distributions in non-
385 uniform aquifer recharge and thickness conditions – An analytical approach based on the
386 assumption of Dupuit-Forchheimer”. **Journal of Hydrology**, 574:110-128,
387 <https://doi.org/10.1016/j.jhydrol.2019.04.032>
- 388 27. Lin, C.C., Chang, Y.C. and Yeh, H.D. (2018) “Analysis of groundwater flow and stream
389 depletion in L-shaped fluvial aquifers”. **Hydrology and Earth System Sciences**,
390 22(4):2359-2375, <https://doi.org/10.5194/hess-22-2359-2018>
- 391 28. Mahdavi, A. (2019) “Transient-state Analytical Solution for Arbitrarily-Located Multiwells
392 in Triangular-Shaped Unconfined Aquifer”. **Water Resources Management**, 33:3615-
393 3631, <https://doi.org/10.1007/s11269-019-02324-6>
- 394 29. Mahdavi, A. (2020) “Steady-state response of annular wedge-shaped aquifers to arbitrarily-
395 located multiwells with regional flow”. **Journal of Hydrology**, 147:103823,
396 <https://doi.org/10.1016/j.jhydrol.2020.124906>
- 397 30. Mahdavi, A. (2021) “Response of dual-zone heterogeneous wedge-shaped aquifers under
398 steady-state pumping and regional flow”. **Advances in Water Resources**, 147:103823,
399 <https://doi.org/10.1016/j.advwatres.2020.103823>
- 400 31. Mahdavi, A. (2022) “Well hydraulics in dual-zone heterogeneous wedge-shaped aquifers
401 under an ambient flow from stream-wise varying boundary heads”. **Journal of Hydrology**,
402 612 (A):128063, <https://doi.org/10.1016/j.jhydrol.2022.128063>

- 403 32. Mahdavi, A. and Yazdani, (2021) “A novel analytical solution for warping analysis of
404 arbitrary annular wedge-shaped bars”. **Archive of Applied Mechanics**, 91:1247-1255,
405 <https://doi.org/10.1007/s00419-020-01858-1>
- 406 33. Malekzadeh, M., Kardar, S. and Shabanlou, S. (2019) “Simulation of groundwater level
407 using MODFLOW, extreme learning machine and Wavelet-Extreme Learning Machine
408 models”, **Groundwater for Sustainable Development**, 9,
409 <https://doi.org/10.1016/j.gsd.2019.100279>
- 410 34. Mallios, Z., Siarkos, I., Karagiannopoulos, P. and Tsiarapas, A. (2022) “Pumping energy
411 consumption minimization through simulation-optimization modelling”, **Journal of**
412 **Hydrology**, 612(A):128062, <https://doi.org/10.1016/j.jhydrol.2022.128062>
- 413 35. Mantoglou, A. (2003) “Pumping management of coastal aquifers using analytical models of
414 saltwater intrusion”. **Water Resources Research**, 39(12),
415 <https://doi.org/10.1029/2002WR001891>
- 416 36. Mohamed, A.M. and Paleologos, E.K. (2018) “Groundwater”. **Fundamentals of**
417 **Environmental Engineering**, <https://doi.org/10.1016/B978-0-12-804830-6.00005-3>
- 418 37. Monachesi, L.B. and Guarracino, L. (2011) “Exact and approximate analytical solutions of
419 groundwater response to tidal fluctuations in a theoretical inhomogeneous coastal confined
420 aquifer”. **Hydrogeology Journal**, 19:1443-1449, <https://doi.org/10.1007/s10040-011-0761->
421 [y](https://doi.org/10.1007/s10040-011-0761-y)
- 422 38. Moutsopoulos, K.N. and Tsihrintzis, V.A. (2005) “Approximate analytical solutions of the
423 Forchheimer equation”. **Journal of Hydrology**, 309(1-4):93-103,
424 <https://doi.org/10.1016/j.jhydrol.2004.11.014>

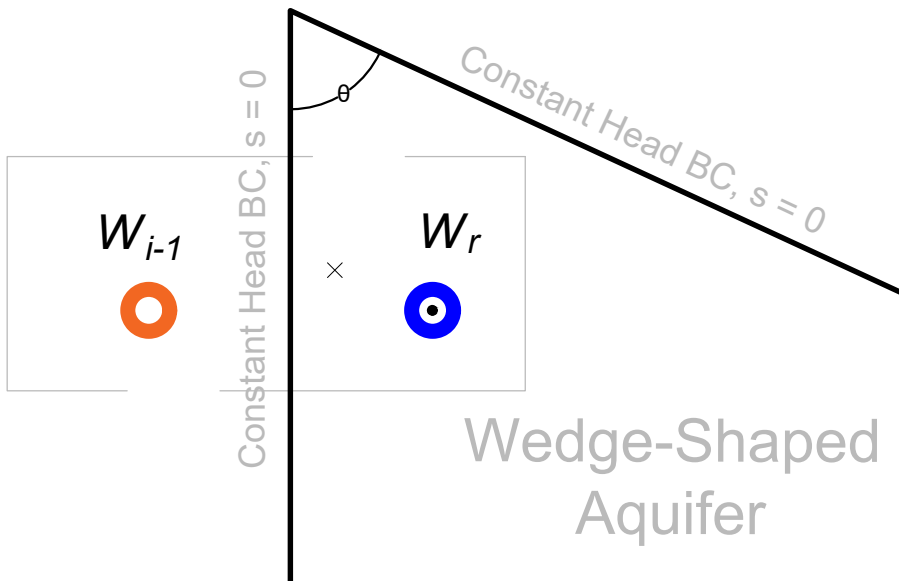
- 425 39. Nagheli, S., Samani, N. and Barry, D.A. (2020) “Capture zone models of a multi-well
426 system in aquifers bounded with regular and irregular inflow boundaries”. **Journal of**
427 **Hydrology X**, 7:100053, <https://doi.org/10.1016/j.hydroa.2020.100053>
- 428 40. Nguyen, K. and Mehrabian, A. (2021) “Capture zone models of a multi-well system in
429 aquifers bounded with regular and irregular inflow boundaries”. **Physical Mesomechanics**,
430 24:20-31, <https://doi.org/10.1134/S1029959921010045>
- 431 41. Nikoletos, I.A. (2020) “Analytical Solutions of Intermittent Transient Groundwater
432 Pumping Cost”. **Journal of Hazardous Toxic and Radioactive Waste**, 24(4),
433 [https://doi.org/10.1061/\(ASCE\)HZ.2153-5515.0000544](https://doi.org/10.1061/(ASCE)HZ.2153-5515.0000544)
- 434 42. Nikoletos, I.A. and Katsifarakis, K.L. (2022) “Approximate application of the method of
435 images in fields with two boundaries intersected at angles between 180° and 90° ”. **Journal**
436 **of Hydrology**, 607:127519, <https://doi.org/10.1016/j.jhydrol.2022.127519>
- 437 43. Okuyade, W.I., Abbey, T.M. and Abbey, M.E. (2022) “Application of the Dupuit–
438 Forchheimer model to groundwater flow into a well”. **Modeling Earth Systems and**
439 **Environment**, 8:2359-2367, <https://doi.org/10.1007/s40808-021-01224-2>
- 440 44. Penny, G., Mullen, C., Bolster, D., Huber, B. and Muller, M.F. (2020) “anem: A Simple
441 Web-Based Platform to Build Stakeholder Understanding of Groundwater Behavior”.
442 **Groundwater**, 59(2):273-280, <https://doi.org/10.1111/gwat.13043>
- 443 45. Rodriguez-Pretelin, A. and Nowak, W. (2019) “Dynamic re-distribution of pumping rates in
444 well fields to counter transient problems in groundwater production”. **Groundwater for**
445 **Sustainable Development**, 8:606-616, <https://doi.org/10.1016/j.gsd.2019.02.009>

- 446 46. Samani, N. and Sedghi, M.M. (2015) “Semi-analytical solutions of groundwater flow in
447 multi-zone (patchy) wedge-shaped aquifers”. **Advances in Water Resources**, 77: 1-16
448 <https://doi.org/10.1016/j.advwatres.2015.01.003>
- 449 47. Samani, N. and Zarei-Doudeji, S. (2012) “Capture zone of a multi-well system in confined
450 and unconfined wedge-shaped aquifers”. **Advances in Water Resources**, 39: 71-84
451 <https://doi.org/10.1016/j.advwatres.2012.01.004>
- 452 48. Sedghi, M.M., Samani, N. and Sleep, B. (2012) “Boundary depletion rate and drawdown in
453 leaky wedge-shaped aquifers”. **Hydrological Processes**, 26(20):3101-3113
454 <https://doi.org/10.1002/hyp.8338>
- 455 49. Sedghi, M.M., Samani, N. and Sleep, B. (2010) “Three-Dimensional Semianalytical
456 Solutions of Groundwater Flow to a Well in Fractured Wedge-Shaped Aquifers”. **Journal**
457 **of Hydrologic Engineering**, 15(12) [https://doi.org/10.1061/\(ASCE\)HE.1943-
458 5584.0000269](https://doi.org/10.1061/(ASCE)HE.1943-5584.0000269)
- 459 50. Sedghi, M.M. and Zhan, H. (2022) “On the discharge variation of a qanat in an alluvial fan
460 aquifer”. **Journal of Hydrology**, 610:127922 <https://doi.org/10.1016/j.jhydrol.2022.127922>
- 461 51. Singh, S.K. (2001) “Identifying Impervious Boundary and Aquifer Parameters from Pump-
462 Test Data”. **Journal of Hydrolic Engineering**, 127(4),
463 [https://doi.org/10.1061/\(ASCE\)0733-9429\(2001\)127:4\(280\)](https://doi.org/10.1061/(ASCE)0733-9429(2001)127:4(280))
- 464 52. Smerdon, B.D., Payton Gardner, W., Harrington, G.A. and Tickell, S.J. (2012) “Identifying
465 the contribution of regional groundwater to the baseflow of a tropical river (Daly River,
466 Australia”. **Journal of Hydrology**, 464-465:107-115,
467 <https://doi.org/10.1016/j.jhydrol.2012.06.058>

- 468 53. Sun, J., Li, J., Liu, Q. and Zhang H. (2011) “Approximate Engineering Solution for
469 Predicting Groundwater Table Variation During Reservoir Drawdown on the Basis of the
470 Boussinesq Equation”. **Journal of Hydrologic Engineering**, 16(10)
471 [https://doi.org/10.1061/\(ASCE\)HE.1943-5584.0000372](https://doi.org/10.1061/(ASCE)HE.1943-5584.0000372)
- 472 54. Teloglou, I.S. and Bansal, R.K. (2012) “Transient solution for stream–unconfined aquifer
473 interaction due to time varying stream head and in the presence of leakage”. **Journal of**
474 **Hydrology**, 428-429:68-79, <https://doi.org/10.1016/j.jhydrol.2012.01.024>
- 475 55. Theim, G. (1906). Hydrologische methoden. Gebhardt, Leipzig, 56.
- 476 56. Wang, L., Dai, C. and Xue, L. (2018) “A Semi-analytical Model for Pumping Tests in
477 Finite Heterogeneous Confined Aquifers With Arbitrarily Shaped Boundary”. **Water**
478 **Resources Research**, 54(4):3207-3216 <https://doi.org/10.1002/2017WR022217>
- 479 57. Winston, R.B. (2009) “ModelMuse-A graphical user interface for MODFLOW-2005 and
480 PHAST” U.S. Geological Survey Techniques and Methods 6-A29, 52 p.
- 481 58. Winston, R.B. (2020) “ModelMuse version 4.3: U.S. Geological Survey Software Release,
482 16 August 2020”. <https://doi.org/10.5066/P9XMX92F>
- 483 59. Yang, S.Y., Huang, C.S., Liu, C.H. and Yeh, H.D. (2014) “Approximate Solution for a
484 Transient Hydraulic Head Distribution Induced by a Constant-Head Test at a Partially
485 Penetrating Well in a Two-Zone Confined Aquifer”. **Journal of Hydraulic Engineering**,
486 140(7) [https://doi.org/10.1061/\(ASCE\)HY.1943-7900.0000884](https://doi.org/10.1061/(ASCE)HY.1943-7900.0000884)
- 487 60. Yeh, H.D. and Chang, Y.C. (2006) “New analytical solutions for groundwater flow in
488 wedge-shaped aquifers with various topographic boundary conditions”. **Advances in**
489 **Water Resources**, 29(3):471-480 <https://doi.org/10.1016/j.advwatres.2005.06.002>

- 490 61. Yeh, H.D. and Chang, Y.C. and Zlotnik, V.A. (2008) “Stream depletion rate and volume
491 from groundwater pumping in wedge-shape aquifers”. **Journal of Hydrology**, 349(3-
492 4):501-511 <https://doi.org/10.1016/j.jhydrol.2007.11.025>
- 493 62. Zipper, S.C., Gleeson, T., Kerr, B., Howard, J.K., Rohde, M.M., Carah, J. and Zimmerman,
494 J. (2019) “Rapid and Accurate Estimates of Streamflow Depletion Caused by Groundwater
495 Pumping Using Analytical Depletion Functions”. **Water Resources Research**, 55(7):5807-
496 5829 <https://doi.org/10.1029/2018WR024403>
- 497 63. Zlotnik, V.A., Kacimov, A. and Al-Maktoumi, A. (2017) “Estimating Groundwater
498 Mounding in Sloping Aquifers for Managed Aquifer Recharge”. **Groundwater**, 55(6):797-
499 810 <https://doi.org/10.1111/gwat.12530>
- 500 64. Zlotnik, V.A., Toundykov, D. and Cardenas, M.B. (2015) “An Analytical Approach for
501 Flow Analysis in Aquifers with Spatially Varying Top Boundary”. **Groundwater**,
502 53(2):335-341 <https://doi.org/10.1111/gwat.12205>
- 503

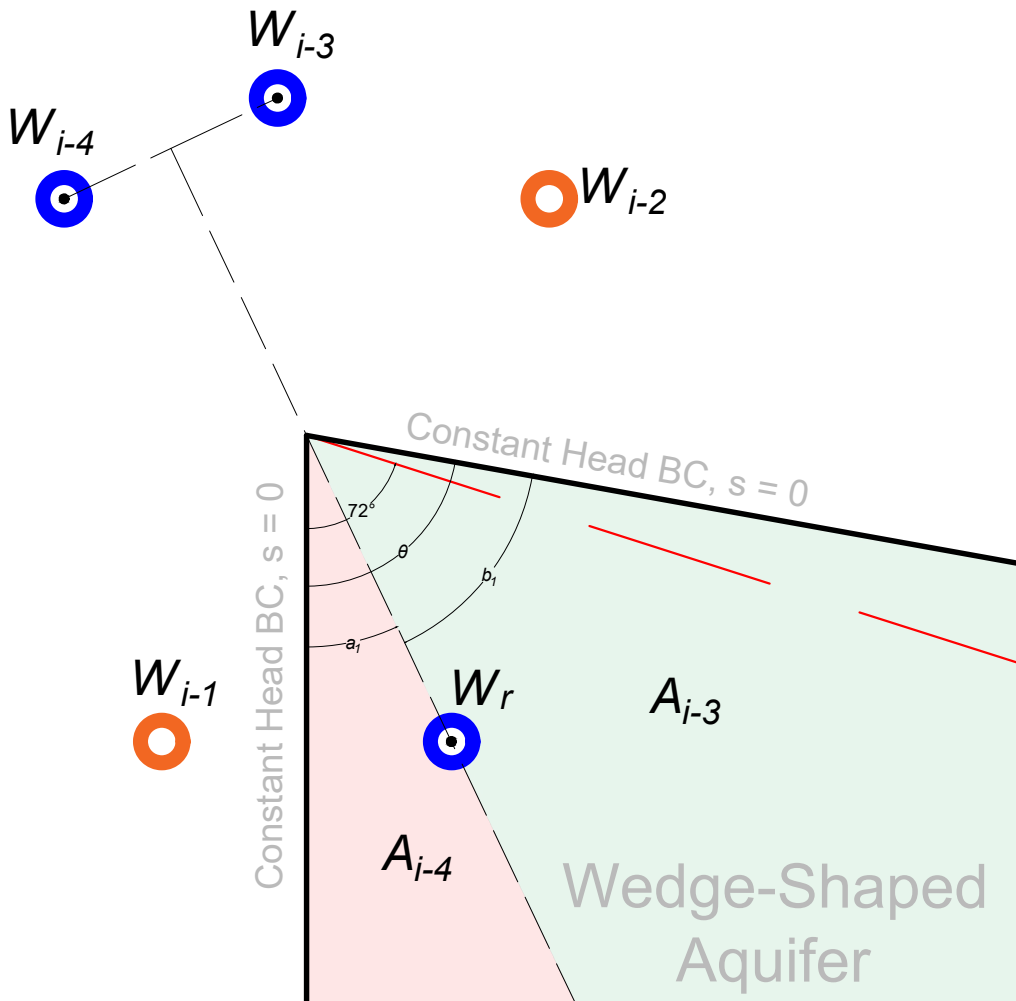
Figure 1.



Explanations

-  Pumping Well
-  Injection Well
- W_r Real Well
- W_i Image Well
- θ Intersecting angle

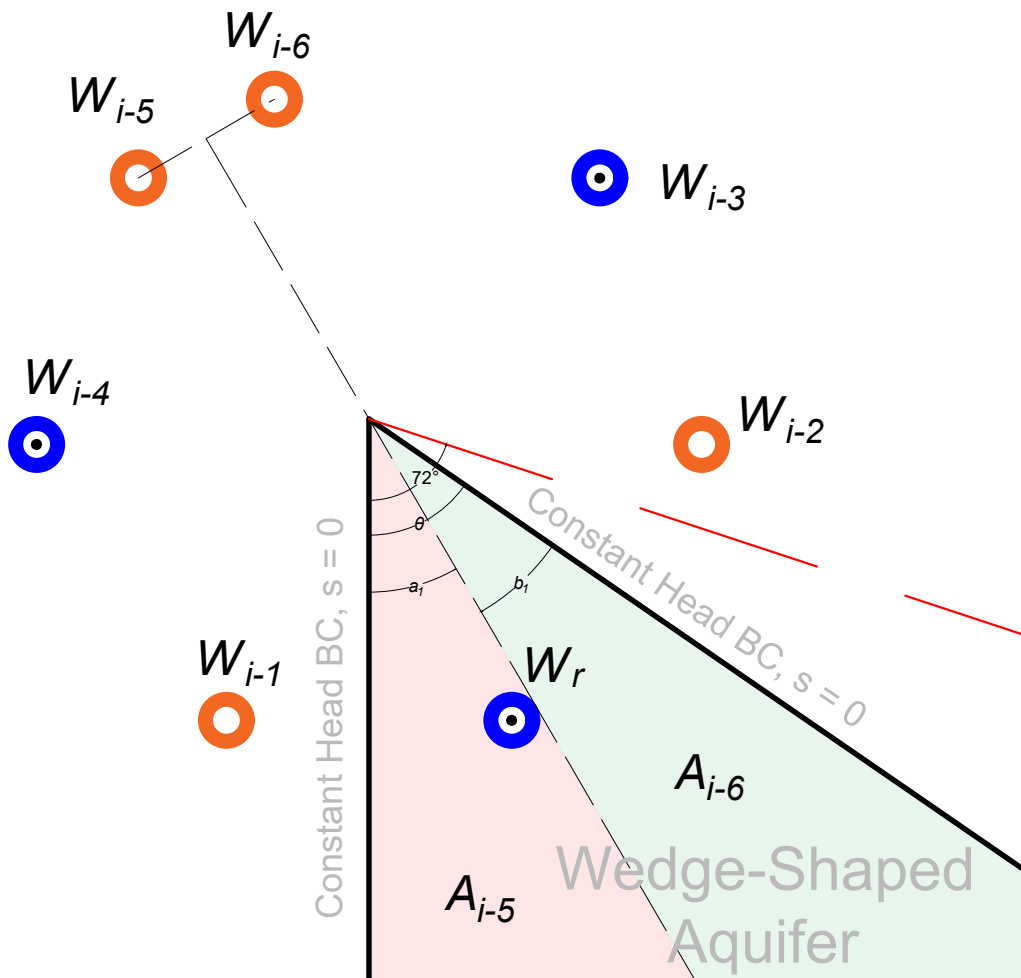
Figure 2.



Explanations

-  Pumping Well
-  Injection Well
- W_r Real Well
- W_i Image Well
- A_{i-3} Red Area
-  Operation of W_{i-3}
- A_{i-4} Red Area
-  Operation of W_{i-4}
- θ Intersecting angle
-  Critical angle 72°

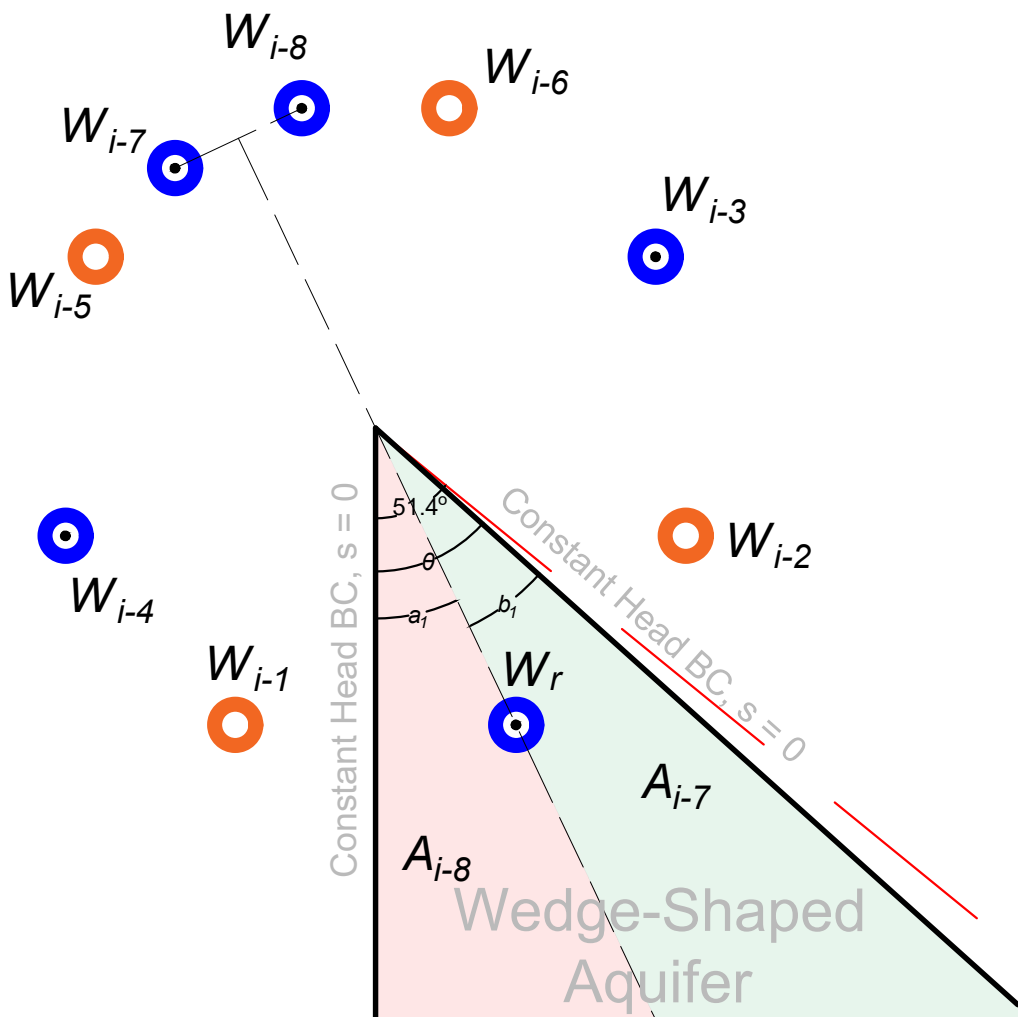
Figure 3.



Expansions

-  Pumping Well
-  Injection Well
- W_r Real Well
- W_i Image Well
- A_{i-5} Red Area
-  Operation of W_{i-5}
- A_{i-6} Red Area
-  Operation of W_{i-6}
- θ Intersecting angle
-  Critical angle 72°

Figure 4.



Explanations

-  Pumping Well
-  Injection Well
- W_r Real Well
- W_i Image Well
- A_{i-7} Red Area
-  Operation of W_{i-7}
- A_{i-8} Red Area
-  Operation of W_{i-8}
- θ Intersecting angle
-  Critical angle 51.4°

Figure 5.

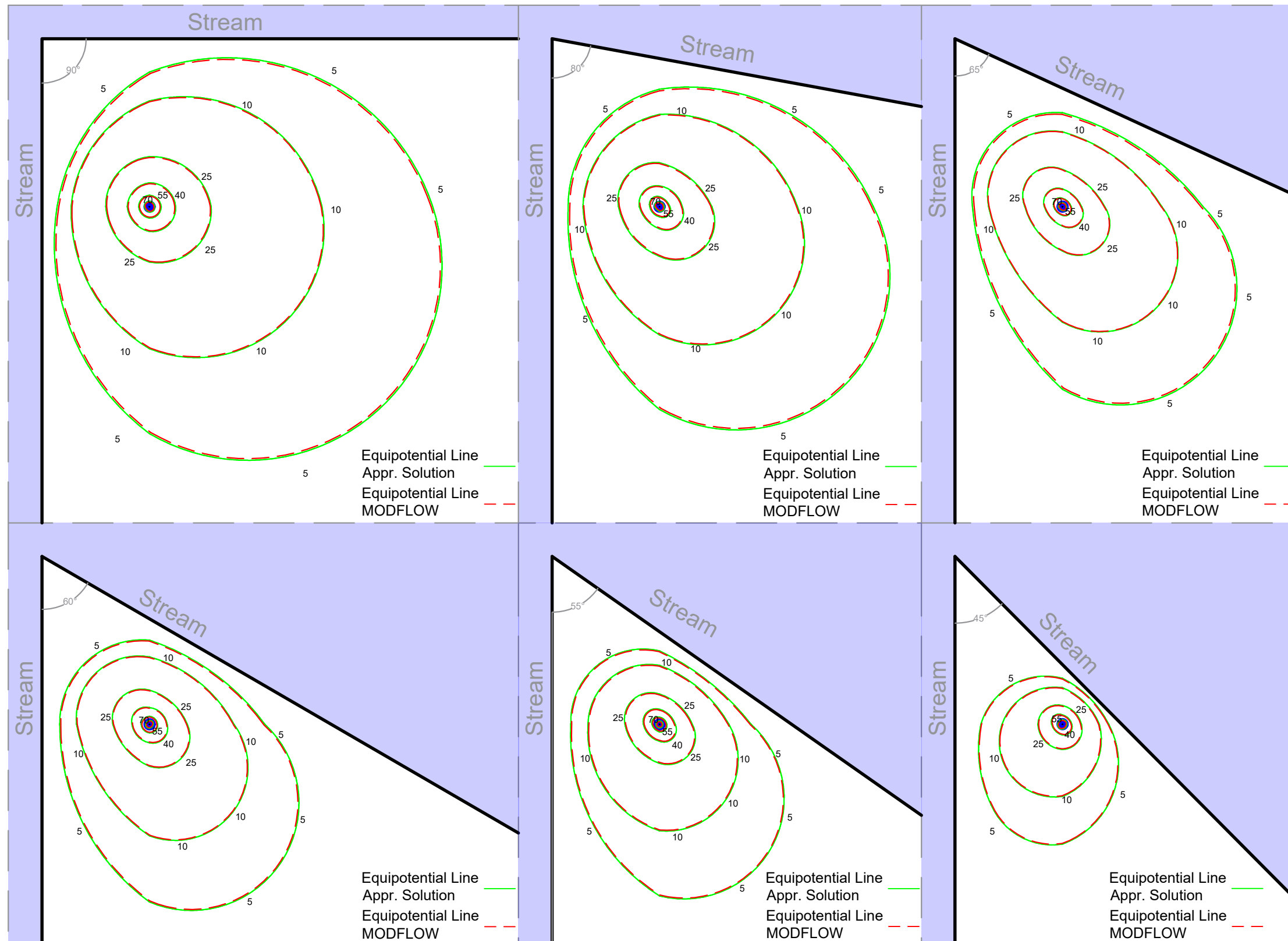


Figure 6.

